Quantum Annealing for Complex Optimization in Satellite Communication Systems

Thinh Q. Dinh *Member, IEEE*, Son Hoang Dau *Member, IEEE*, Eva Lagunas *Senior Member, IEEE*, Symeon Chatzinotas *Fellow, IEEE*, Diep N. Nguyen *Senior Member, IEEE*, and Dinh Thai Hoang *Senior Member, IEEE*

***Abstract*—Satellite communication (SatCom) systems play a vital role in providing global connectivity and enable a wide range of applications, including Internet of Things (IoT) connectivity for remote areas such as forests and oceans. Two crucial resource allocation challenges in SatCom are Beam Placement (BP) and Frequency Assignment (FA) problems, which involve the clique cover (CC) and graph coloring (GC) problems, respectively. Conventional solutions for these problems incur excessive computational cost, which is intractable for classical computers. A promising approach is to formulate these problems using the Ising model, construct their Hamiltonians, and then solve them efficiently by a quantum computer. However, the current quantum computers have very limited hardware and can only handle rather small inputs. To overcome this limitation, we propose a hybrid quantum-classical computational pipeline where an efficient Hamiltonian Reduction method is the key for solving large CC/GC instances. Through experiments on real quantum computers, our reduction method outperforms commercial solutions, allowing quantum annealers to handle significantly larger BP/FA instances while maintaining high probability to achieve feasible solutions and near-optimal performance. Although the inherent hardness of the CC/GC problems cannot be overcome by quantum computing, our research contributes to the early exploration of quantum computing in the context of the complex optimization problems in SatCom systems, particularly in the realm of IoT connectivity for remote areas.**

***Index Terms*—Beam Placement, Quantum Computing, Satellite Communication, Low Earth Orbit**

I. Introduction

Satellite communication (SatCom) systems have become indispensable part of modern civilizations, enabling various applications from telecommunications to Earth observation, including Internet of Things (IoT) connectivity for remote areas like forests and oceans [1]. Low-Earth Orbit (LEO) satellites have emerged as a promising technological solution to extend connectivity and complement the coverage of Geostationary (GEO) satellites [2]. In the context of LEO satellites, the Beam Placement (BP) problem seeks to optimally allocate satellite beams to users, requiring adaptive decision adjustments compared to GEO satellites' fixed beam grids [1]. To simplify the network, operators often need to minimize the number of generated on-board beams [3], [4]. Additionally, the Frequency Assignment (FA) problem looks for optimal frequency-to-beam allocations that minimize frequency resource usage while mitigating interference between nearby beams [3].

The BP and FA problems can be formulated into clique cover (CC) and graph coloring (GC) in graph theory, respectively [3], [5]. This mapping allows express the problems' proximity characteristics. For BP, nearby users can be represented by vertices connected by edges in a graph. The objective is to find the minimum number of cliques (fully connected subsets) that cover all vertices, corresponding to the minimum number of beams [3]. Similarly, for FA, nearby beams cannot share the same frequency, as no adjacent vertices have the same color. The objective is to assign the minimum number of colors (frequencies) [3]. Notably, the CC problem in a graph can be translated into the GC problem in its complement graph [6]. Both CC and GC are NP-hard, meaning that it is intractable for classical computers to efficiently solve all instances unless P = NP [6].

Quantum computers, which process data with quantum bits (or *qubits*) and can simultaneously explore multiple quantum states using superposition, offer a potentially revolutionary approach to address computationally intensive problems [7]. Early theoretical studies have demonstrated promising successes, e.g., Grover's algorithm for speeding up unstructured search problems [8] and Shor's algorithm for breaking Rivest–Shamir–Adleman (RSA) encryption [9].

Quantum processors are typically categorized into two main types: quantum gate processors, from IBM, IonQ, and Rigetti [10], and quantum annealers, manufactured by D-Wave [11]. While the former was developed for general-purpose quantum computers, the latter was specifically designed to tackle combinatorial optimization problems. Currently, quantum annealers possess a sufficient number of qubits to handle a range of real-world applications, from computer sciences, quantum chemistry to protein folding [12]. To utilize quantum computers for optimization tasks, such problems are reformulated as Quadratic Unconstrained Binary Optimization (QUBO) or Ising formulations [13], which can be represented by their Hamiltonians, i.e. the matrices underlying Ising formulations. According to Adiabatic Quantum Optimization theories, Hamiltonians represent the mathematical models of the

Manuscript received 2 May 2024; revised 4 August 2024; accepted 25 September 2024. editor coordinating the review of this article and approving it for publication was H. Zhao. (Corresponding author: Thinh Dinh.)

Thinh Dinh is with the Information System Lab, University of Information Technology, Linh Trung, Thu Duc, Ho Chi Minh City 700000, Vietnam and is also with Vietnam National University Ho Chi Minh City, Linh Trung, Thu Duc, Ho Chi Minh City 700000, Vietnam. E-mail: thinhdq@uit.edu.vn. (Corresponding Author)

Hoang Dau is with the School of Computing, Royal Melbourne Institute of Technology, Australia. E-mail:sonhoang.dau@rmit.edu.au.

Eva Lagunas and Symeon Chatzinotas are with the Interdisciplinary Centre for Security, Reliability and Trust, University of Luxembourg, 2721 Esch-sur-Alzette, Luxembourg. E-mail: {eva.lagunas, Symeon.Chatzinotas}@uni.lu.

Diep Nguyen and Hoang Dinh are with the School of Electrical and Data Engineering, University of Technology Sydney, Australia. E-mail: {Diep.Nguyen, Hoang.Dinh}@uts.edu.au.

problems and are tailored to leverage the unique capabilities of quantum computing [13].

However, quantum annealers are limited by the size of the problem that can be solved. Even with more than 5000 physical qubits, the D-Wave Advantage processors are only able to tackle Quadratic Assignment Problems with 145 or fewer variables [14], [15]. Due to the lack of all-to-all connectivity between the physical qubits in existing quantum annealing hardware, it is often more than one physical qubit is needed to represent a single logical qubit in the original problem's Ising Hamiltonian. This process is called Minor Embedding [16]. Existing techniques like Roof Duality [11], [17] and FastHare [18] to reduce Hamiltonians have limitations, as they work best on sparse Hamiltonians and did not consider constrained optimizations as well. However, many common problems in practice, such as those formulated as CC and GC, are constrained problems.

In this study, we first present the QUBO formulations of CC and GC. Then, we present a hybrid quantum-classical pipeline for solving medium-scale CC and GC problems, both with and without knapsack constraints. This pipeline consists of a Hamiltonian Reduction (HR) method and a corresponding solution reconstruction method. To tackle quantum annealers' limit on the number of variables, rather than using the Hamiltonian from the Ising/QUBO formulation of an original CC/GC problem, our proposed HR method aims to construct a small-size "equivalent" Hamiltonian. There are three steps in our reduction: graph decomposition, presolving variables, and Hamiltonian formulation. In the first step, we decompose a graph into connected components. The second step, which is applied to each connected component, finds large independent sets and then uses linear programming relaxations to presolve most variables of a CC/GC instance. Finally, in the third step, a reduced Hamiltonian is constructed by utilizing the remaining (unsolved) variables, which is subsequently fed into quantum annealers. From their output, we reconstruct the solution to the original CC/GC problem.

To demonstrate the effectiveness of our Hamiltonian Reduction method on BP and FA instances, we conducted experiments and benchmarked our proposed quantum-classical pipeline on several performance metrics. We utilize actual US vessel position data and the assumption that each single ship has a satellite communication subscription. We first demonstrate that our proposed method can typically presolve more than 99% and 87% variables for BP and FA instances, whereas D-Wave Roof Duality can presolve none.

Note that while existing quantum computers are designed to solve QUBOs that are unconstrained, the CC and GC problems are constrained (by the set of edges of the graph). Therefore, when transforming CC or GC into a QUBO, the feasibility of quantum computers' solutions in the original problems may not be guaranteed. In our experiments, the proposed method was able to retain the feasibility of the final solutions at 91.5% while enabling D-Wave Advantages to tackle CC problems with sparse graphs that have 125 times more variables than D-Wave's limit. Our method also enables D-Wave Advantages to tackle GC problems with sparse graphs that have 7 times more variables than D-Wave's variable limit while keeping the final solutions' 97.7% feasibility.

Last but not least, to evaluate the quality of quantum optimization techniques' solutions, prior studies obtained optimal solutions from classical solvers before comparing with quantum solutions [19]–[21]. However, with NP-Hard problems like CC and GC, this approach were limited to work with instances having a small number of variables. In this work, rather than comparing to exact classical solutions, we derive a new way to obtain tight lower bounds of the optimal solutions. Thus, it is more efficient to evaluate quantum solutions.

The major contributions of this work are summarized below.

1) We first propose a novel hybrid quantum-classical computational pipeline to address the Beam Placement (BP) and Frequency Assignment (FA) optimization problems in satellite communication (SatCom) systems. To overcome the hardware limitations of quantum annealers, which make it challenging to solve large-scale optimization instances using quantum annealing alone, the key ingredient of the proposed pipeline is its Hamiltonian Reduction method. This method consists of three steps: isolating connected components, finding a large independent set, and linear programming relaxation.
2) To efficiently evaluate the optimality gaps of solutions from various approaches without the time-consuming search for exact optimal solutions, we employ a new lower bound for those BP and FA problems which is faster to obtain.
3) Finally, we evaluate our approach on synthetic datasets (Erdős-Rényi graphs) and on an actual US vessel position dataset. On the random graphs, our method achieves significant reduction compared to existing reductions approaches such as Roof Duality [11], Symmetric Reduction [22], and Monomial Reduction [22]. On the US vessel position dataset, our method can reduce the size of the original problem by 87% and 99% for the FA and BP instances, respectively. We also observe that the solution quality of our pipeline is comparable to Simulated Annealing and Tabu Search when the size of the reduced problem is at most 40 (variables).

The rest of the paper is organized as follows. Section II discusses related work. Quantum Annealing and the QUBO/Ising formulation are introduced in Section IV. Then, Section III-C presents CC and GC formulations and how to convert them into QUBO formulations. Next, we introduce our Hamiltonian Reduction method in Section V. Section VI shows numerical results. Final conclusions are discussed in Section VII.

II. Related Works

BP and FA are challenging problems for operators in LEO satellite systems as they seek to minimize the number of beams generated onboard while maximizing the gain provided to users and mitigating interference. Recent works [3], [4] on BP face a trade-off between these objectives. Specifically, they assume the use of "Earth Moving Beams" [23], that require agile handover procedures to maintain seamless connectivity for stationary users while the beams are moving with the LEO satellites' motion. They proposed to use greedy approaches

to solve problems whose optimality gap increases as the size of the optimization increases. To achieve better performance, the state-of-the-art solutions for the FA and BP problems in SatCom are computationally complex [24]–[27]. Tedros *et al.* [24] proposed to apply Difference-of-Convex-Functions (DC) and Successive Convex Approximation (SCA) to handle the non-convexity of FA problems in GEO systems; while Bui *et al.* [26] proposed a two-stage algorithm to joint optimize beam placement and load balancing problems in Non-Geostationary (NGSO) satellite systems or Pachler *et al.* proposed to use Particle Swarm Optimization (PSO) to solve the joint power and bandwidth allocation problem in GEO systems [27]. Given the fast dynamic of LEO satellites systems, it is required to obtain fast solutions with near-optimal performance.

Since BP and FA problems can be formulated as Clique Covering (CC) and Graph Coloring (GC) problems, as shown in [28], [29], no polynomial approximation methods for CC and GC can achieve a better approximation ratio than $|V|^{1/7-\epsilon}$ for a general graph with $|V|$ vertices and a small error ϵ. This implies that the gap between a solution achieved by any polynomial-time algorithm and the optimal value increases with $|V|$. Thus, to achieve better performance, more complex approaches like Particle Swarm [27] or Simulated Annealing [30] have been considered in the literature, which often have long convergence time to reduce the gap with the optimal solutions. Given the short communication duration between LEO satellites and Earth users, which is from 5 to 15 minutes due to high velocity of satellites [31], there is an urgent need for faster computational methods. With the capacity of breaking RSA code which is intractable for classical computers, this paper aims at exploring the potential of applying computing in solving BP and FA.

One potential approach to reduce the size of Hamiltonians is Roof Duality [17], a linear relaxation-based approach that lowers the number of unknown variables by partially presolving a subset of binary variables. This approach, included in the D-Wave Ocean SDK [11], is the most renowned Hamiltonian Reduction method. Recently, a new approach known as FastHare was proposed, which seeks non-separable groups of unknowns that share the same values in the optimal solution [18]. However, extensive experiments in [18] showed that the two approaches worked well on some QUBO instances, but not others. Importantly, these approaches were specifically developed for unconstrained QUBO formulations, while the CC and GC problems involve constraints. Thus, the feasibility of these approaches for solving the original CC or GC problems must be investigated further. An early work [22] proposed Symmetrical Reduction method for GC's QUBO formulations. However, experimental results on random graphs in [22] showed that on average Symmetrical Reduction method exceed the current D-Wave hardware limit as the number of vertices of graph is greater than 7.

Another promising approach is to decompose the original problems into multiple sub-QUBOs. An early method, D-Wave's Qbsolv [11] decomposes large QUBO instances into smaller ones, then sequentially optimizes each sub-QUBO, before finding the final solutions using Tabu-search [11]. However, this approach does not guarantee optimality and Tabu-search is computationally costly. Bender decomposition and Alternating Direction Method of Multipliers (ADMM) have also been proposed to deal with constrained mixed-integer linear problems (MILP) [32], [33]. However, the numbers of binary variables in sub-QUBOs may not be smaller than those in the original MILP. Graph decomposition/reduction techniques have shown promising results for specific graph problems. Authors partitioned/reduced large graph instances of specific problems such as partitioning large Max-Cut instances [21] and leveraging DBK (Decomposition, Bounds, k-core) to split large Maximum Clique problems [34] into smaller subgraphs before transforming them into QUBOs then sending them to quantum computers.

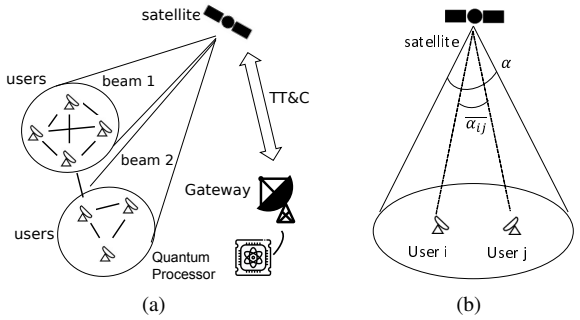

Fig. 1: (a) Illustration of a LEO system and (b) An example of two users served by one satellite beam.

III. System Model and Problem Formulation

In this section, we describe a system model in SatCom where Beam Placement (BP) and Frequency Assignment (FA) are optimized sequentially. Then, we introduce how these problems are formulated as Clique Cover (CC) and Graph Coloring (GC) problems.

A. SatCom Beam Placement

Consider a LEO system, illustrated in Fig. 1(a), consisting of satellite with an antenna array and N users. The satellite is capable of providing a maximum of B beams, where B is less than or equal to the total number of users in the system[1]. The BP involves assigning a set of satellite beams to a set of user nodes in order to provide communication coverage. We represent the set of user indices as $\mathcal{N} = \{1, \ldots, N\}$ and the set of beam indices as $\mathcal{B} = \{1, \ldots, B\}$. The satellite is connected to a High Performance Computer (HPC) equipped with a quantum processor through its TT & C (telemetry, tracking, and control) link for optimization operations. Here, each user must be associated with one beam. Furthermore, the network operator tries to reduce the number of onboard-generated beams while maintaining the required service for its subscribers in order to take advantage of users' traffic diversity

[1]We assume the standard setting in which a beam can serve multiple users and a user can be served by at most one beam (see, e.g. [3], [24], [26]). We also assume that users have uniform demands. The case of non-uniform demands is an open problem for future research.

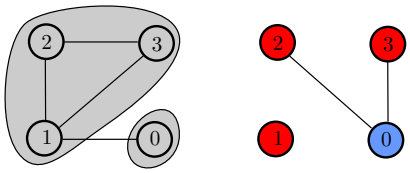

Fig. 2: (a) a clique cover on a given graph G and (b) its equivalent graph coloring on the complement graph $\bar{G}$.

and optimize multicast benefits [3], [4]. To achieve that, network operators could serve proximate satellite communication subscribers with the same beam.

This problem can be modeled as a CC problem, where each beam represents a clique, and the nodes covered by a beam form the vertices of the corresponding clique.

In order to construct the *proximity graph* for CC, previous studies [3], [26] have shown that for a given set of users to be served by the same beam, they must be separated by an angle $\bar{\alpha} \leq \frac{\alpha}{2}$, where α represents the cone angle of a beam (see Fig. 1(b)). Therefore, given a set of users' locations, different undirected proximity graphs $G_t = (V_t, E_t)$ are generated based on the satellite's position in the sky during different time slots t. An edge between user u and user v exists in the graph if $\bar{\alpha}_{uv} \leq \frac{\alpha}{2}$. Moreover, each beam can serve no more than W users.

B. SatCom Frequency Assignment

The next step for the operator is to assign frequencies to the beams aiming at minimizing the frequency resources required, while also ensuring that neighboring beams are assigned distinct frequencies to mitigate inter-beam interference. This is equivalent to solve a GC problem where a *conflict graph* is constructed based on the positions of the beam centers. In this graph, an edge is established between two beams if the angle between their centers, denoted as β_{uv}, is less than or equal to twice the cone angle $\beta_{uv} \leq 2\alpha$. This angle constraint guarantees that two nearby beams should have assigned different frequencies to avoid interference.

C. Clique Cover and Graph Coloring Formulation

Clique Cover (CC) and Graph Coloring (GC) problems are two equivalent problems in graph theory. CC seeks the minimum number of cliques required to cover all vertices, while GC aims to minimize the number of colors needed to color all vertices without adjacent vertices sharing the same color. They are equivalent because a minimum clique cover for a graph G corresponds to a minimum coloring of its complement $\bar{G}$ and vice versa [6] (as illustrated in Fig. 2).

In this paper, we use two versions of the CC and GC problems: with and without constraints on the maximum number of members in a clique or the maximum number of vertices that can share the same color. The former, which involves constraints, is commonly referred to as the bounded version of the problems. This can be applied into the SatCom BP problems. On the other hand, the latter is the unbounded ones, which can be applied into SatCom FA problems. We formally describe both versions below.

Given an undirected graph $G = (V, E)$, where V is the set of nodes and E is the set of edges, the decision variables z_c and a_{uc} represent whether clique/color c is used and whether vertex u is assigned to clique/color c, respectively. We use the Node Association Matrix (NAM), which is defined as $\mathbf{A} = (a_{uc}) \in \{0, 1\}$, where $a_{uc} = 1$ if node u is assigned to clique/color c. Otherwise, $a_{uc} = 0$. The set $\mathcal{C} \triangleq \{1, 2, \ldots, |V|\}$ represents the indices of cliques/colors the nodes are assigned to. Note that a trivial clique cover/coloring consists of $|V|$ different cliques/color classes of size one. We re-use W to represent the maximum size of each clique/color in the bounded version of the GC/CC problems. By minimizing the objective function, the problem aims to find the minimum number of cliques to cover all vertices in the graph G, or equivalently, to find the minimum number of colors needed to color its complement graph $\bar{G}$.

$$\text{P1: } \min_{z_c, a_{uc}} \sum_{c \in \mathcal{C}} z_c, \tag{1}$$

$$\text{s.t. C1: } \sum_{c \in \mathcal{C}} a_{uc} = 1, \forall u \in \mathcal{N}, \tag{2}$$

$$\text{C2: } a_{uc} \leq z_c, \forall u \in \mathcal{N}, \forall c \in \mathcal{C}, \tag{3}$$

$$\text{C3: } a_{uc} + a_{vc} \leq 1, \forall c, \text{if}(u, v) \notin G, \tag{4}$$

$$\text{C4: } \sum_{u \in \mathcal{N}} a_{uc} \leq W, \forall c \in \mathcal{C}, \tag{5}$$

$$\text{C5: } z_c, a_{uc} \in \{0, 1\}. \tag{6}$$

As indicated by C1, each node must be associated with a single clique or color. The constraint C2 guarantees that no node can be a member of a unused clique or color. The constraint C3 ensures two nodes that are not neighbors in G (or, equivalently, are neighbors in $\bar{G}$) should belong to different cliques (or colors). The constraint C4 enforces the maximum possible number of members assigned to a clique (or a color). By removing C4, we obtain the unbounded version of the GC/CC problem.

Due to the NP-Hardness of GC/CC, it is intractable to solve them on classical computers [6]. Thus, in next section, we introduce about the background of Quantum Annealing, its current limitations and how to build a hybrid quantum-classical pipeline to efficiently solve those problems.

IV. Quantum Annealing and QUBO/Ising Formulation

Quantum annealers, especially D-Wave, leverage the quantum mechanical nature of a physical system of S qubits to solve optimization problems [11], [13]. Here, Hamiltonians determine the energy profile of the quantum system. According to Adiabatic Quantum Optimization theories [13], the quantum system is initiated at the ground state $|\psi_0\rangle$ of the original Hamiltonian H_0 and then gradually evolves to the ground state $|\psi_P\rangle$ of the desired Hamiltonian H_P over a given long duration T as follows.

$$\mathcal{H}(t) = \left(1 - \frac{t}{T}\right) H_0 + \frac{t}{T} H_P, \tag{7}$$

TABLE I: Key notations used in the paper

Notation	Definition
i, j	index of qubits
H_0, H_P	the initial and targeted Hamiltonian
S	number of qubits in a physical system
$\mathcal{N}$	the set of nodes
$G, \bar{G}$	the graph and its complement
u, v	the indices of nodes in the graph
c	the index of cliques
$\deg(v)$	the degree of node v
z_c	0/1-valued, indicating whether the clique/color c is used or not
a_{uc}	0/1-valued, indicating if node u belongs to clique/color c or not
W	the maximum number of nodes per clique

where,

$$H_0 = \sum_{i=1}^{S} \sigma_i^x, H_P = \sum_{i=1}^{S} f_i \sigma_i^z + \sum_{i,j=1}^{S} F_{ij} \sigma_i^z \sigma_j^z. \quad (8)$$

In (8), f_i and F_{ij} are the *coupler strength* and *bias parameters*, respectively, while σ_i and σ_i are Z and X Pauli operations on the ith qubit, respectively [13]. By measuring the system's ground state at time T, we might discover the optimal solution of an equivalent Ising model such that

$$\min_{s_i \in \{-1,1\}^S} H_P(\mathbf{s}) = \sum_{i=1}^{S} f_i s_i + \sum_{i,j=1}^{S} F_{ij} s_i s_j. \quad (9)$$

An alternate formulation of the Ising model is a Quadratic Unconstrained Binary Optimization (QUBO):

$$\min_{\mathbf{x} \in \{0,1\}^S} \quad \sum_{i=1}^{S} Q_{ii} x_i + \sum_{i,j=1}^{S} Q_{ij} x_i x_j, \quad (10)$$

where $\mathbf{x} = [x_1, \ldots, x_S]$ are binary variables and $\mathbf{Q} \in \mathbb{R}^{S \times S}$ is an upper triangular matrix. It is simple to switch between QUBO and an Ising model by mapping $s_i = 2x_i - 1$, $f_i = \frac{1}{2} Q_{ii} + \frac{1}{4} \sum_{j=1}^{S} Q_{ij} + \frac{1}{4} \sum_{j=1}^{S} Q_{ji}$ and $F_{ij} = \frac{1}{4} Q_{ij}$.

A. QUBO Transformation

The problem P1 can be transformed into QUBO based on prior knowledge of how to include constraints into the objective as quadratic penalties as follows [13]. First, binary slack variables $s_{cw}, w \in \mathcal{W} = \{1, \ldots, W\}$ are introduced to turn C4 into equalities. Then, we transform P1 into $\overline{\text{P1}}$ defined as follows.

$$\overline{\text{P1}}: \min_{\substack{\{z_c\}, \{a_{uc}\}, \\ \{s_{cw}\}}} \sum_{c \in \mathcal{C}} z_c, \quad (11)$$

$$\text{s.t.} \quad (2) - (4), (6)$$

$$\sum_{u \in \mathcal{N}} a_{uc} + \sum_{w \in \mathcal{W}} w s_{cw} = W, \forall c \in \mathcal{C}. \quad (12)$$

Let $\mathbf{x} = [\mathbf{a}_1^T, \ldots, \mathbf{a}_{|\mathcal{C}|}^T, z_1, \ldots, z_{|\mathcal{C}|}, \mathbf{s}_1, \ldots, \mathbf{s}_{|\mathcal{C}|}]^T$ represent the variables of $\overline{\text{P1}}$ in a column vector. We define matrices $\mathbf{Q}_{C1}, \mathbf{Q}_{C2}, \mathbf{Q}_{C3}$ and $\mathbf{Q}_{C4}$ corresponding to constraints C1, C2, C3, and C4, respectively. Additionally, we define matrix $\mathbf{Q}_o$ corresponding to the objective function. The rules for converting traditional constraints into corresponding penalties are described in Table II (see [35] for a more detailed treatment). The QUBO problem is formulated as follows.

TABLE II: Rules for Converting Constraints to Penalties

Constraint	Equivalent Penalty
C1: $a_1 + a_2 + a_3 = 1$	$\lambda(a_1 + a_2 + a_3 - 1)^2$
C2: $a \leq z$	$\lambda(a - az)$
C3: $a_1 + a_2 \leq 1$	$\lambda(a_1 a_2)$
C4: $\sum_u a_u + \sum_w w s_w = W$	$\lambda(\sum_u a_u + \sum_w w s_w - W)^2$

$$\text{QUBO}: \min_{\mathbf{x}} \quad \mathbf{x}^T \mathbf{Q} \mathbf{x}, \quad (13)$$

where $\mathbf{Q} = \mathbf{Q}_o + \lambda\big(\mathbf{Q}_{C1} + \mathbf{Q}_{C2} + \mathbf{Q}_{C3} + \mathbf{Q}_{C4}\big)$. Here, λ is a constant that controls the relative importance of satisfying the constraints versus minimizing the objective function, and

$$\mathbf{Q}_o = \text{diag}\Big(\Big[\mathbf{0}_{1 \times (|V||\mathcal{C}|)}, \mathbf{1}_{1 \times |\mathcal{C}|}, \mathbf{0}_{1 \times (W|\mathcal{C}|)}\Big]\Big), \quad (14)$$

$$\mathbf{Q}_{C1} = \mathbf{K}_1^T \mathbf{K}_1 - 2\text{diag}\Big(\mathbf{d}_1^T \mathbf{K}_1\Big), \quad (15)$$

$$\mathbf{Q}_{C2} = \text{diag}\Big(\Big[\mathbf{1}_{1 \times (|V||\mathcal{C}|)}, \mathbf{0}_{1 \times (|\mathcal{C}| + W|\mathcal{C}|)}\Big]\Big) + \begin{bmatrix} \mathbf{0}_{|V||\mathcal{C}| \times |V||\mathcal{C}|}, & \mathbf{K}_2, & \mathbf{0}_{|V||\mathcal{C}| \times W|\mathcal{C}|} \\ \mathbf{0}_{(|\mathcal{C}| + W|\mathcal{C}|) \times |V||\mathcal{C}|}, & \mathbf{0}_{(|\mathcal{C}| + W|\mathcal{C}|) \times |\mathcal{C}|}, & \mathbf{0}_{(|\mathcal{C}| + W|\mathcal{C}|) \times W|\mathcal{C}|} \end{bmatrix}, \quad (16)$$

$$\mathbf{Q}_{C3} = \text{diag}\Big(\Big[\underbrace{\overline{\mathbf{F}}, \ldots, \overline{\mathbf{F}}}_{|\mathcal{C}| \text{ times}}, \mathbf{O}_{(|\mathcal{C}| + W|\mathcal{C}|) \times (|\mathcal{C}| + W|\mathcal{C}|)}\Big]\Big), \quad (17)$$

$$\mathbf{Q}_{C4} = \mathbf{K}_3^T \mathbf{K}_3 - 2\text{diag}\Big(\mathbf{d}_2^T \mathbf{K}_3\Big), \quad (18)$$

where $\mathbf{d}_1$, $\mathbf{K}_1$, $\mathbf{d}_2$, $\mathbf{K}_2$, $\mathbf{K}_3$ are derived later in (19)-(20). In this context, $\mathbf{I}$ denotes the identity matrix and $\overline{\mathbf{F}}$ is the $|V| \times |V|$ adjacency matrix of the complement of G. The function $\text{diag}(\cdot)$ creates a matrix with its argument on the main diagonal. Following [13], we set λ equal to $|\mathcal{C}| + 1$. In the unbounded version, we remove the last $W|\mathcal{C}|$ columns and rows in $\mathbf{Q}_o, \mathbf{Q}_{C1}, \mathbf{Q}_{C2}$, and $\mathbf{Q}_{C3}$, which represent C4. We also set $\mathbf{Q}_{C4} = 0$ in that case.

To make $\mathbf{Q}$ an upper-triangular matrix, which can then be used by D-Wave solvers, we modify it by setting $Q_{ij} = Q_{ij} + Q_{ji}, \forall j > i$ and $Q_{ij} = 0, \forall j < i$.

B. Scaling Limitations of Current Hardware

To construct QUBO, quantum computers require $|\mathcal{C}||V| + |V| + W|\mathcal{C}|$ logical qubits for solving P1. Current quantum computers, including D-Wave, require more than 5000 physical qubits to represent fewer than 145 logical qubits [15]. For example, an input with $|V| = 10$, $|\mathcal{C}| = 10$, and $W = 3$, which requires 140 logical qubits, can be handled by D-Wave Advantage. However, it can no longer handle a slightly larger input with 13 nodes and 13 cliques/colors, where each clique/color can cover 5 nodes, which requires 247 logical qubits, exceeding D-Wave's capacity.

C. A Case Study of How Quantum Annealing Solves the Clique Cover Problem

In this section, we present a case study to demonstrate how to use D-Wave's quantum annealing to solve a CC instance.

$$\mathbf{d}_1 = \mathbf{1}_{|V|\times 1}, \quad \mathbf{d}_2 = W\mathbf{1}_{|V|\times 1}, \quad \mathbf{K}_1 = [\underbrace{\mathbf{I}_{|V|\times|V|}, \ldots, \mathbf{I}_{|V|\times|V|}}_{|\mathcal{C}| \text{ times}}, \mathbf{0}_{|V|\times|\mathcal{C}|}, \mathbf{0}_{|V|\times W}], \tag{19}$$

$$\mathbf{K}_2 = \begin{bmatrix} -\mathbf{1}_{|V|\times 1}, & \mathbf{0}_{|V|\times 1}, \ldots, & \mathbf{0}_{|V|\times 1} \\ \mathbf{0}_{|V|\times 1}, & -\mathbf{1}_{|V|\times 1}, \ldots, & \mathbf{0}_{|V|\times 1} \\ & \vdots & \\ \underbrace{\mathbf{0}_{|V|\times 1}, \; \mathbf{0}_{|V|\times 1}, \; \ldots, -\mathbf{1}_{|V|\times 1}}_{|\mathcal{C}| \text{ columns}} \end{bmatrix}, \mathbf{K}_3 = \begin{bmatrix} \mathbf{1}_{1\times|\mathcal{C}|} & \mathbf{0}_{1\times|\mathcal{C}|} & \cdots & \mathbf{0}_{1\times|\mathcal{C}|} & \mathbf{0}_{1\times|\mathcal{C}|} & 1\cdots W & \mathbf{0}_{1\times W} & \mathbf{0}_{1\times W} & \cdots & \mathbf{0}_{1\times W} \\ \mathbf{0}_{1\times|\mathcal{C}|} & \mathbf{1}_{1\times|\mathcal{C}|} & \cdots & \mathbf{0}_{1\times|\mathcal{C}|} & \mathbf{0}_{1\times|\mathcal{C}|} & \mathbf{0}_{1\times W} & 1\cdots W & \mathbf{0}_{1\times W} & \cdots & \mathbf{0}_{1\times W} \\ \vdots & \vdots & \ddots & \vdots & \vdots & \vdots & \vdots & \vdots & \ddots & \vdots \\ \mathbf{0}_{1\times|\mathcal{C}|} & \mathbf{0}_{1\times|\mathcal{C}|} & \cdots & \mathbf{1}_{1\times|\mathcal{C}|} & \mathbf{0}_{1\times|\mathcal{C}|} & \mathbf{0}_{1\times W} & \mathbf{0}_{1\times W} & \mathbf{0}_{1\times W} & \cdots & 1\cdots W \end{bmatrix}. \tag{20}$$

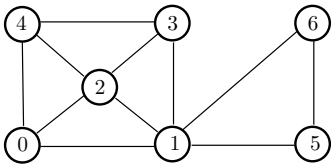

Fig. 3: An example of a graph of seven vertices, which can be covered (optimally) by three cliques.

We consider a graph with 7 vertices and 9 edges (see Fig. 3), and aim to find a minimum number of cliques that can cover all the vertices of this graph. We assume no limit on the size of each clique. We apply the D-Wave's quantum annealing function to this graph with different annealing times and observe the lowest energy found by the annealer. As shown in Fig. 4, when the number of anneals increases, the energy of the quantum system decreases. When the energy is sufficiently low, the solutions returned by the annealer are *feasible*. Additionally, as the number of anneals increases to 3000, we can obtain an *optimal* clique cover (three cliques).

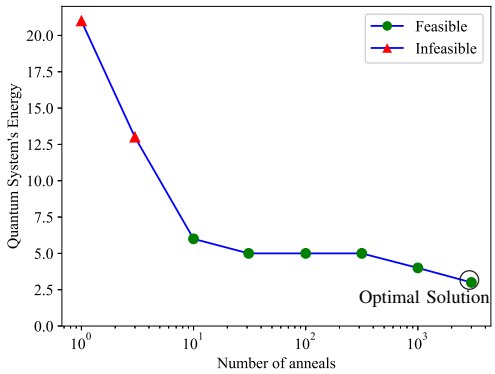

Fig. 4: Performance of D-Wave on Clique Cover on a small instance. As the system's energy[2]gets sufficiently low, the quantum annealer starts to return feasible solutions, eventually reaching the optimality.

V. A Novel Hybrid Quantum-Classical Pipeline

This section proposes a hybrid quantum-classical computational pipeline to solve CC/GC instances. As the coloring problem on a graph can be transformed into the clique cover problem on the complement graph, we will mainly describe our pipeline using the clique cover problem for succinctness. Our pipeline first reduces the original Hamiltonian into smaller ones, and then feeds them into quantum annealers. The returned outputs can be used to reconstruct solutions for the original problem. More specifically, the graph is first decomposed into connected components, where solutions for each component suffice for the entire graph (see Remarks 1 and 2). Then, the variable presolve technique is utilized to identify a large independent set in each component. As such nodes cannot belong to the same cliques, they can be assigned to different cliques to further reduce the number of input variables (i.e. the vertex-to-clique variables a_{uc}). After this initial assignment, in each connected component, we formulate P2, which is a reduced version of P1 that aims to assign the remaining nodes to as few cliques as possible (including the cliques containing the nodes in the aforementioned independent set). The linear relaxation of P2 is then solved to assign several nodes to their respective cliques. Finally, a reduced Hamiltonian is constructed, and a quantum computer is employed to find clique allocations for the unassigned nodes in each connected component.

A. Graph Decomposition

Before solving a CC or GC problem, it is essential to isolate connected components in the given graph. This is because finding a solution on the original graph is equivalent to finding solutions for the CC/GC problem on all connected components, which have smaller sizes and are easier to solve. Let $\text{MCC}(G)$ and $\chi(G)$ denote the size of a minimum clique cover of a graph G and the minimum number of colors required to color the vertices of G.

Remark 1. *Let $G = (V, E)$ be a graph with connected components $G_{(1)}, \ldots, G_{(K)}$, where $G_{(k)} = (V_{(k)}, E_{(k)})$. The size of a minimum clique cover of G is equal to the sum of the sizes of the minimum clique covers of its connected components, i.e., $MCC(G) = \sum_{k=1}^{K} MCC(G_{(k)})$.*

Remark 2. *The minimum number of colors to color G is equal to the maximum among the minimum numbers of colors required to color its connected components, i.e., $\chi(G) = \max_{k=1,\ldots,K} \chi(G_{(k)})$.*

[2]The D-Wave quantum annealing system does not directly return energies in physical units like Joules or electronVolts. Instead, it works with dimensionless quantities called "arbitrary units" (AU) in its calculations [36]. The energy values in the results take the form of relative values in these arbitrary units, ranking the quality of different possible solutions [36].

Algorithm 1 Find an independent set

Input: $G = (V, E)$ - the undirected input graph
Output: V_{ind} - an independent set of G
1: $V_{\text{ind}} = \emptyset$,
2: **while** $V \neq \emptyset$ **do**
3: $v^* = \arg\min_{v \in V} \deg(v)$,[2]
4: $V_{\text{ind}} = V_{\text{ind}} \cup \{v^*\}$,
5: $V = V \setminus (\{v^*\} \cup \Gamma(v^*))$,[2]
6: **end while**

B. Two-step Variable Presolve

1) Find a Large Independent Set: In this step, our pipeline finds a large independent set in G and pre-assigns nodes in that set to different cliques. Note that finding a maximum independent set in a graph is known to be computationally challenging and falls under the category of NP-hard problems. As an alternative, approximation methods from literature such as the one proposed by Boppana and Halldórsson [37] can be employed. In our study, as a proof-of-concept, we use a simple yet efficient greedy algorithm (see Algorithm 1) to find a large independent set, denoted V_{ind}. As nodes in every independent set must belong to different cliques in any clique cover, we can then assign nodes in V_{ind} to $|V_{\text{ind}}|$ different cliques/colors without loss of optimality. This step presolves $|V_{\text{ind}}| \times |\mathcal{C}|$ variables a_{uc} (with u belongs to the independent set V_{ind}) from the problem formulation P1.

More formally, after pre-assigning nodes u_ℓ's in $V_{\text{ind}} = \{u_\ell\}_{\ell=1}^{|V_{\text{ind}}|}$ to $|V_{\text{ind}}|$ different cliques c_ℓ's, we can formulate a reduced problem P2, with the last constraint only using the subgraph induced by the set of the remaining vertices $V \setminus V_{\text{ind}}$.

$$\text{P2: } \min_{z_c, a_{uc}} \sum_{c \in \mathcal{C}} z_c, \tag{21}$$

$$\text{s.t. } (2) - (5),$$

$$a_{u_\ell c_\ell} = 1, \ \ell = 1, \ldots, |V_{\text{ind}}|, \tag{22}$$

$$a_{u_\ell c_{\ell'}} = 0, \ \ell' \neq \ell, \ell = 1, \ldots, |V_{\text{ind}}|, \tag{23}$$

$$z_{c_\ell} = 1, \ \ell = 1, \ldots, |V_{\text{ind}}|, \tag{24}$$

$$z_c, a_{uc} \in \{0, 1\}, \forall u \in V \setminus V_{\text{ind}}. \tag{25}$$

Lemma 1. *Let* $\text{OPT}(P1)$ *and* $\text{OPT}(P2)$ *denote the optimal values of P1 and P2, respectively. Then,* $\text{OPT}(P1) = \text{OPT}(P2)$.

Proof. The optimality of the clique cover is unaffected by pre-assigning the nodes in an independent set to different cliques (indices) because these non-adjacent nodes cannot belong to the same cliques. □

2) Linear Programming Relaxation: In this step, we consider the linear relaxation P2′ of P2 given below. Recall that we already assign node u_i's to the clique c_ℓ's for all $u_\ell \in V_{\text{ind}}$ - the independent set found in the previous step.

$$\text{P2}' : \min_{z_c, a_{uc}} \sum_{c \in \mathcal{C}} z_c, \tag{26}$$

$$\text{s.t. } (2) - (5), (22) - (24),$$

$$z_c, a_{uc} \in [0, 1], \forall u \in V \setminus V_{\text{ind}}. \tag{27}$$

[2] $\deg(v)$ is the degree of node v; $\Gamma(v)$ is the set of neighbors of node v.

Algorithm 2 Hybrid Quantum-Classical Pipeline

Input: $G = (V, E)$, W (optional), problem type (Clique Cover or Graph Coloring)
Output: $\mathbf{x}^{\text{QA}}$ - a solution to P1
1: Decompose G into connected components $G_{(k)}$.
2: **for** each $G_{(k)}$ **do**
3: **if** problem type is Clique Cover **then**
4: Find an independent set of $G_{(k)}$ using Algo. 1.
5: Compute an optimal solution $\bar{\mathbf{x}}_{(k)}$ of P2′ on $G_{(k)}$.
6: Form $Q_{(k)}$, $\bar{V}_{(k)}$ - the set of unassociated nodes of $G_{(k)}$.
7: Form $Q'_{(k)}$ by selecting rows and columns of $Q_{(k)}$ corresponding to $z_c, c = |\tilde{\mathcal{C}}| + 1, \ldots, \bar{C}$, $a_{ic}, i \in \bar{\mathcal{V}}, c = \tilde{\mathcal{C}} + 1, \ldots, \bar{C}$ and $s_{bw}, w = 1, \ldots, \overline{W}_c, c \in \tilde{\mathcal{C}}$.
8: **else**
9: Perform lines 4-7 on $\bar{G}_{(k)}$.
10: **end if**
11: After transforming $Q'_{(k)}$ to $H'_{P(k)}$, send $H'_{P(k)}$ to D-Wave Advantage processor.
12: After obtaining results from D-Wave, return $\mathbf{x}^{\text{QA}}_{(k)}$, by combining the results of D-Wave with $\bar{\mathbf{x}}_{(k)}$ for G_k.
13: **end for**
14: Aggregate $\mathbf{x}^{\text{QA}}$ from $\mathbf{x}^{\text{QA}}_{(k)}$ by following Remarks 1 and 2.

This problem P2′ can be efficiently solved by the well-known simplex method [38]. The solution of P2′ provides a lower bound on the optimal values of P2 and P1.

Theorem 1. *Denote the optimal value of P1′ and P2′, i.e., the linear relaxation formulations of P1 and P2, by* $\text{OPT}(P1')$ *and* $\text{OPT}(P2')$*, respectively. Then we have* $\text{OPT}(P1') \leq \text{OPT}(P2') \leq \text{OPT}(P2) = \text{OPT}(P1)$.

Proof. First, as the feasible region of P2 is a subset of the feasible region of P1, the same holds for P2′ and P1′, which implies that $\text{OPT}(\text{P1}') \leq \text{OPT}(\text{P2}')$.

Next, we have $\text{OPT}(\text{P2}') \leq \text{OPT}(P2)$, which is due to the fact that P2′ is the linear relaxation formulation of P2. Based on Lemma 1, $\text{OPT}(P1) = \text{OPT}(P2)$. Combining all the above inequalities, the proof of the theorem follows. □

Thanks to the lower bound established in Theorem 1, even without solving P1 or P2 optimally, which is a challenging task, we can still benchmark the performance of our proposed pipeline (see Fig. 10). We also note that it is faster to solve P2′ than P1′ because P2′ has fewer variables. Furthermore, the lower bound obtained by the solution of P2′ is often much tighter than that of P1′.

C. Reduced Hamiltonian Formulation

1) Unbounded Version: After finding an optimal solution $\bar{\mathbf{x}}$ by solving P2′, those nodes u that are associated to the clique/color c (i.e., $a_{uc} = 1$) are placed in that clique/color. The unassociated nodes are grouped in the set $\bar{V}$. The set of used cliques/colors is denoted as $\tilde{\mathcal{C}}$, and due to the symmetry of clique/color variables, it can be re-indexed from 1 to $|\tilde{\mathcal{C}}|$. A reduced version of the QUBO formulated from P1 is constructed as a Hamiltonian.

An upper bound on the number of additional cliques/colors required (other than the first $|\tilde{\mathcal{C}}|$ cliques/colors) is $\bar{C} = \min\{C - |\tilde{\mathcal{C}}|, |\bar{V}|\}$, where C is the maximum number of cliques/colors that can be used (we set $C = |V|$ in our implementation). The reduced Hamiltonian only includes z_c

for $c = |\tilde{\mathcal{C}}| + 1, \ldots, |\tilde{\mathcal{C}}| + \bar{C}$, and a_{uc} for $u \in \bar{\mathcal{V}}$ and $c = |\tilde{\mathcal{C}}| + 1, \ldots, |\tilde{\mathcal{C}}| + \bar{C}$.

For example, consider a graph with three vertices 1, 2, 3, and two edges (1,2) and (2,3). Assume that we have obtained a pre-assignment solution in which node 1 and node 2 are assigned to clique 1. Here, the graph can be formed by a maximum of $C = |V| = 3$ cliques. Since 1 and 2 are assigned, only node 3 is undecided. As a results, the maximum number of additional cliques is $\bar{C} = 1$. Hence, $z_1 = 1$ and $z_3 = 0$. Then, the vector $\mathbf{x} = [1, 0, 0, 1, 0, 0, -, -, -, 1, -, 0]$, where $-$ is an undecided value. Here, the first, second and third group of 3 elements of $\mathbf{x}$ are the association decisions for node 1, node 2, and node 3, respectively. The last 3 elements of $\mathbf{x}$ are indicators whether to use clique 1, 2, and 3, respectively.

2) Bounded Version: The main difference between bounded and unbounded version lies in the presence of slack variables. The slack variables corresponding to used clique/color c are only kept if the number of nodes associated to that clique/color is smaller than W. Denote the vacancies of clique/color c by $\overline{W}_c$. For example, if $W = 5$ and there are two nodes associated with a given clique/color c', the vacancies of c' is 3, i.e, $\overline{W}_{c'} = 3$, we only keep slack variables $s_{c'1}, s_{c'2}$ and $s_{c'3}$. Slack variables corresponding to $c = |\tilde{\mathcal{C}}| + 1, \ldots, \bar{C}$ are set to zero to further decrease the quantities of variables in the reduced Hamiltonian by making the assumption that the size of the largest clique of the remaining nodes is less than or equal to W. It is important to note that if this assumption is not satisfied, the resulting solution becomes infeasible, lowering the success probability of this hybrid quantum-classical computation pipeline (see Fig. 8).

Let $j \in J$ be the set of indices of rows/columns of Q which are related to pre-assigned variables. We have

$$\sum Q_{ii'} x_i x_{i'} + \sum Q_{ii} x_i \tag{28}$$

$$= \sum_{i,i' \notin J} Q_{ii'} x_i x_{i'} + \sum_{i,j \forall x_j = 1} Q_{ij} x_i + \sum_{i,j \forall x_j = 1} Q_{ji} x_i + \sum Q_{ii} x_i + \text{constant} \tag{29}$$

$$= \sum Q'_{ii'} x_i x_{i'} + \sum Q'_{ii} x_i + \text{constant}. \tag{30}$$

To construct the reduced Q', we first change the value of $Q_{ii}, \forall i \notin J$ such that

$$Q_{ii} = Q_{ii} + \sum_{j \in J, x_j = 1} Q_{ij} + \sum_{j \in J, x_j = 1} Q_{ji}. \tag{31}$$

Then, we construct Q' based on rows and columns corresponding to undecided variables. For example in Fig. 5, given an original Q, which is a 12×12 matrix, and vector $\mathbf{x} = [1, 0, 0, 1, 0, 0, -, -, -, 1, -, 0]$, we first revise the diagonal vector of Q. For example, $Q_{77} = 23$ and $Q_{88} = 13$. Then, we construct Q' based on the rows $7, 8, 9$ and 11 with columns $7, 8, 9$ and 11.

After that, for both the unbounded and bound versions, the reduced Hamiltonian H'_P is constructed by the new matrix Q'.

D. Quantum Annealing and Solution Recovery

We then send the reduced Hamiltonian H'_P to quantum processors using the Quantum Cloud Providers' APIs. After receiving the solutions from quantum computers, we combine the solution with the lowest energy level with the ones we obtained from solving P2′ to recover a solution to P1. The complete pseudo-code for this process can be found in Algorithm 2. We note that $Q_{(k)}$ in Algorithm 2 is the matrix Q corresponded to connected component $G_{(k)}$.

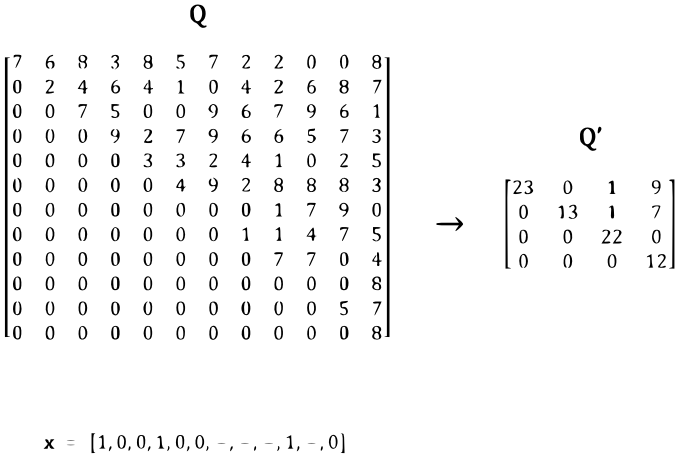

Fig. 5: An example of constructing matrix Q' based on Q and pre-assigned decision $\mathbf{x}$.

TABLE III: Default Parameter Setup.

Parameter	Value
Number of satellite users	25–200
Satellite's altitude	1110 km
Satellite's latitude and longitude	26.812309^o, -85.386382^o
Number of realization	200

To solve a BP instance using the hybrid quantum-classical pipeline, a graph G is first constructed to represent the proximity of users based on their locations. The graph is then decomposed, and a reduced Hamiltonian is created for each resulting subgraph. The quantum annealer receives the Hamiltonian of each subgraph, providing individual solutions, which are then aggregated to recover a solution for the original BP instance.

Similarly, for a FA instance, a conflict graph G is first constructed to represent the inter-beam interference. Then, the graph is decomposed into smaller subgraphs, and the complement of each subgraph is computed to transform the GC problem to the CC problem. The reduced Hamiltonians for the complement subgraphs are then sent to the quantum annealer, and the returned bitstrings are used to recover a solution to the original FA problem.

VI. Numerical Results

In this part, we run simulations to evaluate the performance of the proposed hybrid quantum-classical pipeline. We simulate the satellite subscribers utilizing actual vessel positions recorded by the US Coast Guard on January 1, 2022 [39]. We first conduct BP optimization where each satellite subscriber is treated as a node in the proximity graph used in the bounded CC problem. For each sample size n (the number of users/nodes in the graph) ranging from 25 to 200, we take 200 random samples of locations from identifiable vessels in the

p	V	Original	Roof Dual.	Sym. Reduction	Mono. Reduction	Our Method	p	V	Original	Roof Dual.	Sym. Reduction	Mono. Reduction	Our Method
0.75	3	12	12	10.31	17.20	0.00	0.90	3	12	12	11.35	19.47	0.00
	4	20	20	16.90	30.41	0.00		4	20	20	18.82	35.07	0.00
	5	30	30	145.12	327.76	0.05		5	30	30	170.38	389.19	0.00
	6	42	42	212.62	486.06	0.14		6	42	42	249.12	577.36	0.00
	7	56	56	291.53	673.41	0.33		7	56	56	344.49	803.22	0.02
	8	72	72	384.38	894.23	0.67		8	72	72	454.33	2594.31	0.04
0.80	3	12	12	10.63	17.87	0.00	0.95	3	12	12	11.69	49.87	0.00
	4	20	20	17.52	31.89	0.00		4	20	20	19.40	92.83	0.00
	5	30	30	153.63	348.57	0.03		5	30	30	178.64	989.51	0.00
	6	42	42	224.47	515.08	0.07		6	42	42	259.17	1470.89	0.00
	7	56	56	309.64	717.00	0.15		7	56	56	360.95	2041.47	0.00
	8	72	72	407.97	951.84	0.36		8	72	72	474.11	2722.52	0.01
0.85	3	12	12	10.98	18.64	0.00							
	4	20	20	18.20	33.53	0.00							
	5	30	30	162.28	369.25	0.01							
	6	42	42	237.42	546.97	0.03							
	7	56	56	326.47	758.43	0.08							
	8	72	72	431.16	1007.69	0.16							

TABLE IV: This table shows the average numbers of remaining binary variables over reduction schemes on binomial random graphs. Following the setting in [22], $p \in \{0.75, 0.8, 0.85, 0.9, 0.95\}$ is the probability an edge exists, $V \in \{3, \ldots, 8\}$ is the number of vertices. We compute the average over 10^4 instances for each pair of (p, V). For example, for $p = 0.75$ and $V = 3$, the number of variables in the original QUBO is 12. The average numbers of unsolved variables on 10^4 random graphs after applying Roof Duality, Symmetrical Reduction, and Monomial Reduction are 12, 10.31 and 17.30, respectively, while our pipeline was able to pre-solve all.

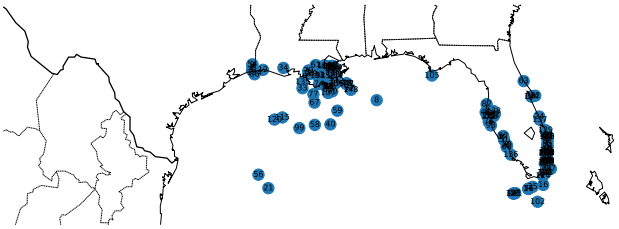

Fig. 6: Positions of 150 randomly selected ships at the southern coast of the U.S.

Gulf of Mexico region. We also choose the most common LEO altitude for Starlink at 1110 km for the satellite's altitude [3]. We set the satellite's latitude at 26.812309^o and its longitude at -85.386382^o. The maximum number of users that can be served by one beam W is 20. Once BP instances are solved, by leveraging the BP centers resulted from those BP instances, we conduct FA optimization where each beam center is treated as a node in an unbounded GC problem. For the D-Wave Quantum Annealing settings, the annealing time is set at the default value of 20μs with 3000 samples. Thus, the total annealing time T is 0.06s. We note that even though the maximum number of anneals is 10000, we found that we can set the number of anneals up to 3000, during the time conducting this research, because D-Wave wants to avoid any users monopolizing their quantum resources [40].

A. Qubit Reduction

In this section, we evaluate the *effectiveness* of our reduction method by comparing the average number of remaining variables corresponding to the reduced Hamiltonians achieved by our method with Symmetric Reduction [22], Monomial Reduction [22], and the function Roof Duality in the D-Wave Ocean SDK [11]. Here, Symmetric Reduction and Monomial Reduction are reduction methods designed for graph coloring instances. Note that the average number of remaining variables corresponding to the Hamiltonians have a direct impact on the complexity of the problem.

1) On Binomial Random Graphs: Following the setting in [22], we first compare our reduction method on small random conflict graphs where the probability of an edge existing increases from 0.75 to 0.95 and the number of vertices $|V|$ increases from 3 to 8. For each pair of (p, V), we generate 10^4 random conflict graphs. Then, we perform our reduction method as well as Roof Duality. For the performance of Symmetric Reduction and Monomial Reduction, we re-use the results mentioned in [22].

As shown in Table IV, our approach achieved significantly smaller average numbers of remaining variables on dense random conflict graphs. This is because with such high edge probability values, the graphs are likely to be complete graphs. As a result, it is likely to find the maximum independent set in the complementary graph consisting of all vertices. Therefore, our method can solve the graph coloring instances prior to constructing the reduced QUBO formulations in most scenarios. We also see that with $V \leq 4$, Symmetrical Reduction method can obtain better performance than Roof Duality. However, as $|V|$ increases, Symmetrical Reduction method introduces many new auxiliary variables. Thus, our approach is more scalable than those in [22] in the parameter range.

2) On Real-World Data: Next, we evaluate our reduction method on US Vessel data. As depicted in Fig. 7, in our experiments, we observed that the D-Wave Roof Duality method did not lead to a noticeable reduction in the number of variables in the Hamiltonian. On the other hand our variable presolve step demonstrated substantial reductions in the size of the Hamiltonian. For example, on BP instances, when the number of users is 200, which is equivalent to 44200 logical

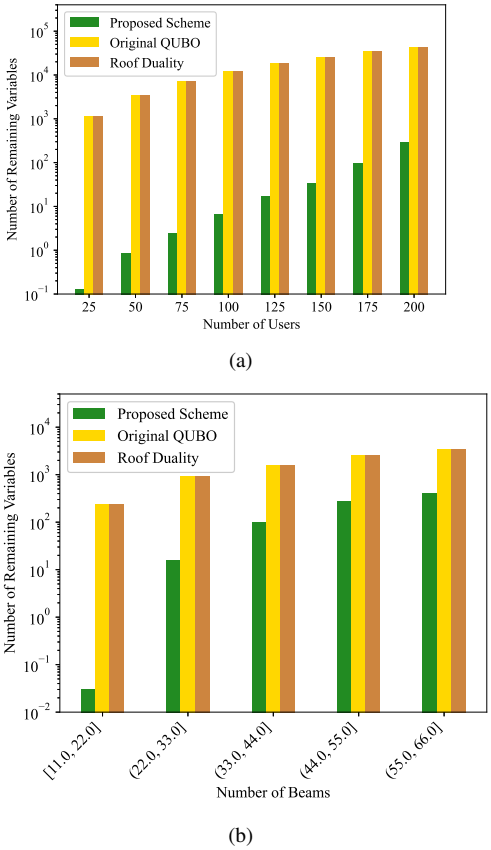

Fig. 7: The average numbers of remaining binary variables in different reduction schemes on (a) BP instances and (b) FA instances.

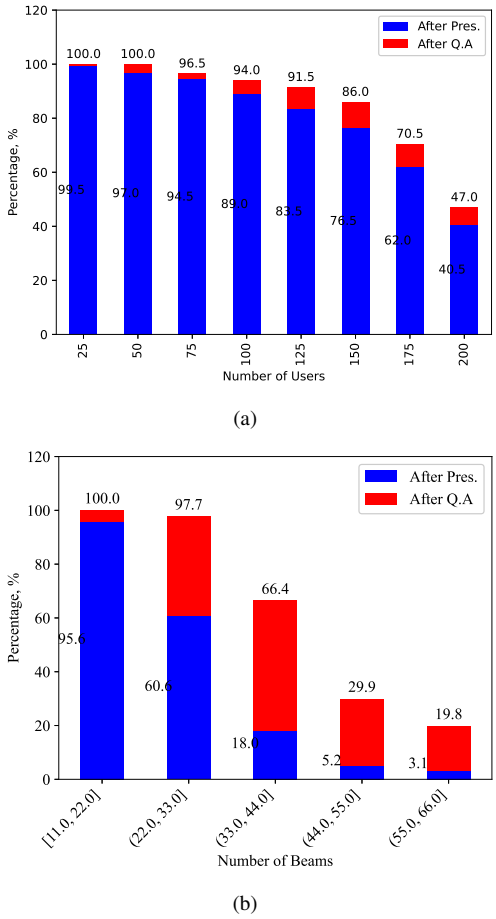

Fig. 8: Success probability to achieve feasible solutions of the proposed hybrid quantum classical pipeline in (a) BP instances and (b) FA instances.

qubits to form H_P, our proposed scheme can reduce to 288.35 logical qubits on average, which corresponds to more than 99% reduction. On FA instances, in the worst case when the number of beams is from 55 to 66, which is equivalent to 3432.20 logical qubits (on average) to form H_P, we need 413.31 logical qubits (on average) on reduction Hamiltonians, which corresponds to more than 87% reduction.

B. Probability To Obtain Feasible Solutions

This section aims to evaluate the probability to obtain feasible solutions through our hybrid quantum-classical pipeline. We use the term *success probability* for the likelihood that the proposed pipeline's solutions are feasible in the original problem P1. There are a few reasons why some solutions may not be feasible after running D-Wave Quantum Annealing. First, the number of anneals is limited due to D-Wave's policy to prevent users from monopolizing their resources. And second, if the size of the reduced Hamiltonian exceeds D-Wave's hardware limit, the instance cannot be solved by D-Wave. Fig. 8 depicts the outcomes depending on various circumstances. The percentage of instances when all nodes are successfully associated to the beams by solving P2′ (the presolve step) without using Quantum Annealing (QA) are depicted by blue color and labeled as "Pres.", demonstrating the performance of our variable presolve approach. Red color is used to represent the percentage of instances in which the presolve step cannot solve all variables and QA must be called.

Our findings indicate that the proposed pipeline successfully resolves a significant number of BP instances with fewer than 125 users. Additionally, we are able to solve an extra 9.5% of the BP instances that the reduction strategy alone cannot address by using QA to handle the undecided variables. On the contrary, we note that the Hamiltonian reduction scheme may not be well-suited for graph coloring instances in the context of Frequency Assignment. As can be seen from Fig. 8 (b), the success probability reduces from 66.4% to 29.9% as the size of the graph increases to more than 44 nodes. This is because the reduction scheme performs better on sparse proximity graphs in Clique Covering context, which are equivalent to dense conflict graphs in the Graph Coloring context. However, the conflict graphs encountered in our experiments are sparse, leading to poor success rates.

It is worth noting that the Binary Quadratic Model (BQM) as well as Constrained Quadratic Model (CQM) implemented in D-Wave fail to solve these BP/FA instances due to the large number of variables involved.

This article has been accepted for publication in IEEE Internet of Things Journal. This is the author's version which has not been fully edited and content may change prior to final publication. Citation information: DOI 10.1109/JIOT.2024.3481373

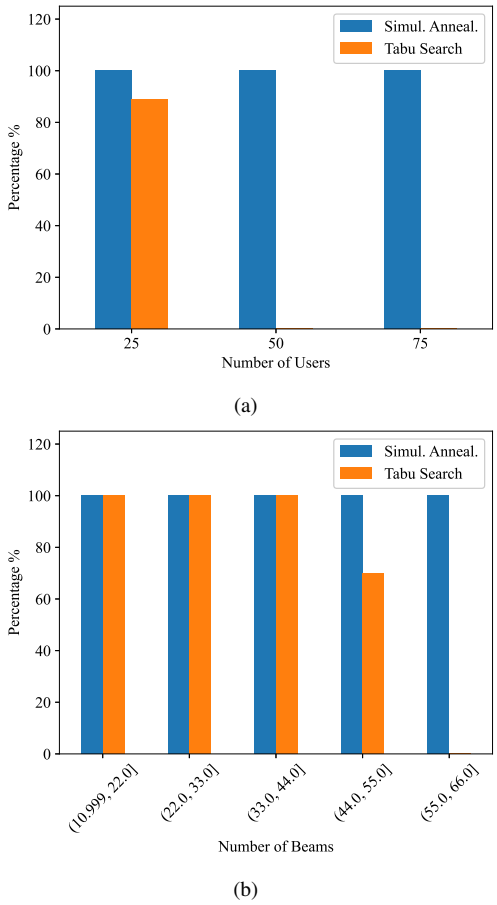

Fig. 9: Success probability to achieve feasible solutions of Simulated Annealing and Tabu Search on (a) BP instances and (b) FA instances.

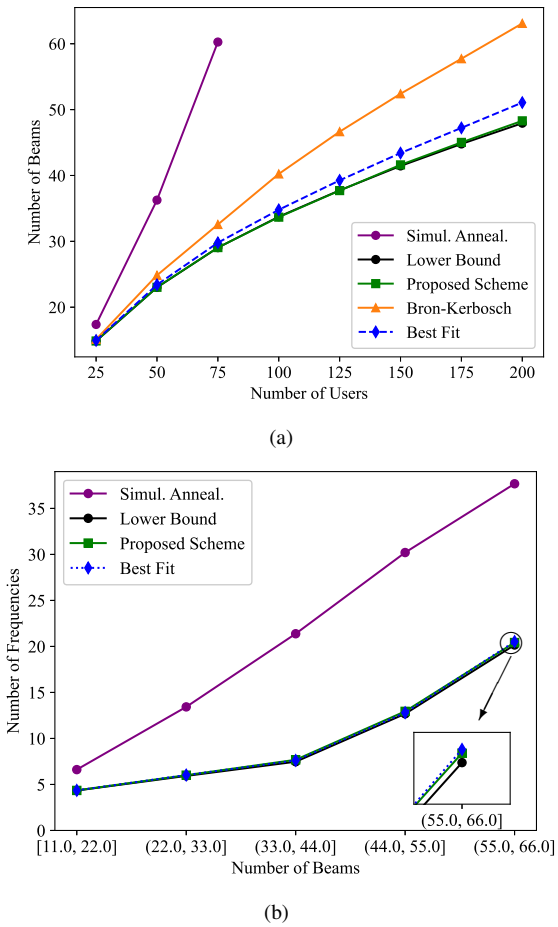

Fig. 10: The performance comparison of our proposed algorithm and various benchmarks, including Bron-Kerbosch, Simulated Annealing, and Best Fit. For the BP problem, our method outperforms other approaches and almost achieves the lower bound. For the FA problem, the solutions obtained by our method are close to the lower bound and Best Fit, and significantly better than Simulated Annealing.

C. Algorithm Performance

In this section, we will assess the performance of our proposed hybrid quantum-classical (HQC) pipeline compared to a range of widely recognized classical algorithms: Tabu Search, Simulated Annealing, Best Fit [41] and Bron-Kerbosch, in the context of BP/FA. We selected Tabu Search and Simulated Annealing because they are well known algorithms and already implemented in D-Wave's SDK, which makes it more convenient to benchmark against our solution. We also picked two classical greedy algorithms, Best Fit and Bron-Kerbosch for two reasons: first, they are classical algorithms for solving resource allocation problems [3], [41], [42], and second, their implementation simplicity and low time complexity fit perfectly into the rapid dynamics of LEO satellite networks[3]. The settings of these algorithms are given below.

- Tabu Search: Utilizing the matrix Q of QUBO, the QUBO formulation of P1, we use it as the input of the Multi-start Tabu Search algorithm [44], which is implemented in the D-Wave Ocean SDK. For a fair comparison with QA, the number of iterations for Multi-start Tabu Search is set at 3000.
- Simulated Annealing: Similar to Tabu Search, we make use of Q as the input of the Simulated Annealing algorithm [45], which is implemented in the D-Wave Ocean SDK. For a fair comparison with QA, the number of iterations for Simulated Annealing is set at 3000.
- Best Fit: A node is simply allocated to the most frequently used clique/color without violating any constraints. If no existing clique/color can accommodate a node, a new clique/color is used by the algorithm.
- The Bron-Kerbosch algorithm [42] is used in [3] to find all maximal cliques in a graph, then greedily union largest cliques until all vertices are covered.

We also note that the input for QA is the reduced Hamiltonian H'_P, or equivalently Q', while the input for Tabu Search and Simulated Annealing is Q which are much larger than Q'.

As shown in Fig. 9, we first observe the success probability of complex algorithms: Tabu Search and Simulated Annealing.

[3]As mentioned in [43], the LEO satellite network setup time, including the network resource allocation, could be in a range of ten seconds to one minute depending on different network operators. Therefore, the beam placement/frequency assignment algorithms employed in the setup phase must be very fast to be practical.

The success probability of Tabu Search suddenly drops to zero as the number of variables is more than 3100, while that of Simulated Annealing remains high. Therefore, when comparing the objective values of algorithms, Tabu Search is excluded due to lack of feasible solutions.

In other words, we want to see how far the solutions obtained by our method are from the optimal in comparisons with other algorithms. In order to ensure a fair evaluation, we only consider cases that are fully solved by Quantum Annealing, excluding instances where the reduction scheme achieves optimality. It is important to note that the performance of the Simulated Annealing exhibits the worst performance in our evaluations due to large number of variables while the number of anneals is fixed at 3000. Additionally, Bron-Kerbosch algorithm obtains the second worst performance over BP instances. We can observe in the following section that Bron-Kerbosch is the fastest algorithm which could explain its low performance.

As can be seen in Fig. 10(a), we observe the divergence trends of Best Fit and Bron-Kerbosch from the lower bound as the number of users (number of vertices $|V|$) in network increases. These results align with the theoretical results in [28], [29], which state that no polynomial approximation can achieve a better approximation ratio than $|V|^{1/7-\epsilon}$ for a general graph with $|V|$ vertices. This implies that the gap between a solution achieved by any polynomial-time algorithm and the optimal value increases with $|V|$. Thus, the gap between such a solution with a lower bound increases as well.

In order to establish a lower bound for the optimal BP, we utilize the objective value of P2$'$ as a reference. The results shown in Fig. 10(a) demonstrates that Quantum Annealing provides feasible solutions that achieve objective values close to the optimal quality in the context of BP instances. Moreover, we observe that as the number of users increases, the performance gap between Quantum Annealing and other benchmarks widens.

On FA instances, we observe that the proposed scheme can achieve near optimal solutions. However, with the network size of up to 66 nodes, Best Fit can also achieve near optimal performance.

D. Computational Time Comparison

In this section, we compare the computational performance of various algorithms, including our proposed quantum-classical pipelines with and without Graph Decomposition (GD), Tabu Search, Simulated Annealing, Best Fit, and the Bron-Kerbosch algorithm. Our evaluation focuses on the computational time required by each approach, which is shown in Fig. 11. Additionally, we also assess the practical usability of these algorithms by comparing them with the communication duration between LEO satellites and Earth users [31], which is from 5 to 15 minutes due to high velocity. Thus, the time to make network decision should be comparably smaller than the duration.

Our proposed quantum-classical pipelines combine both quantum and classical computing resources to solve the problem at hand. When utilizing GD, the performance of the pipeline is enhanced by decomposing the problem into

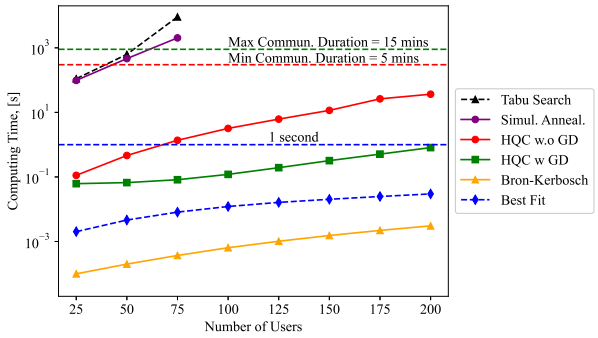

Fig. 11: The computing time comparison of our proposed algorithm, Tabu Search, Simulated Annealing, Bron-Kerbosch, and Best Fit. Our approach requires less time than the first two but more time than the last two.

connected components, which allows for more efficient processing. Comparing the pipelines with and without GD, we find that the GD-based approach exhibits faster computational time, demonstrating the effectiveness of this decomposition technique.

Our method has distinctive advantages compared to other resource allocation algorithms, including Simulated Annealing, Tabu Search, Bron-Kerboch and Best Fit, as explained below. First, as observed in Fig. 11, our method is much faster than Simulated Annealing and Tabu Search, i.e., while ours takes less than 1 second to return a solution for up to 200 users, Simulated Annealing and Tabu Search' running time already exceeds 5 minutes for 50 users. Such expensive running time renders these two methods impractical for LEO satellite applications, as the entire communication duration between the satellites and ground users is usually between 5 and 15 minutes only. On the other hand, while Bron-Kerboch and Best Fit run faster, their solutions, especially those of Bron-Kerboch, are not as close to the optimal solutions as those solutions returned by our pipeline (see Fig. 10a). Note that the main step that makes our method slower than Bron-Kerboch and Best Fit is the preprocessing, which includes solving the Linear Programming Relaxation P2$'$.

VII. Conclusion

In this paper, we explored the application of quantum computing to solve the Clique Cover (CC) and Graph Coloring (GC) problems within satellite communication networks, specifically focusing on the instances of Beam Placement (BP) and Frequency Assignment (FA) problems with respect to a practical dataset of vessel locations in the United States. Initially, we derived a Quadratic Unconstrained Binary Optimization (QUBO) formulation suitable for quantum annealers as input. Due to quantum annealers' hardware limitation, we then introduced a Hamiltonian reduction technique to reduce the number of necessary logical qubits. Our proposed method obtained remarkable performance by significantly reducing the number of required logical qubits compared to the Roof Duality technique in D-Wave's library, which provides no reduction. Furthermore, our experimental results highlighted the high probability of achieving feasible solutions employing

our reduction method in conjunction with Quantum Annealing. In comparison, both D-Wave's Binary Quadratic Model (BQM) and Constraint Quadratic Model (CQM) struggled to solve instances involving more than 145 variables. Notably, our proposed approach outperformed Best Fit, a renowned classical approach. This research demonstrated a promising advancement in leveraging quantum computing for encompassing CC and GC formulations, especially their applications in SatCom for IoT connectivity at remote areas. We expect that our contribution will inspire future exploration of quantum computers in tackling conventionally known NP-hard problems.

Last but not least, our Hamiltonian reduction approach for BA and FA can be widely applied into other applications of Clique Covering (CC) and Graph Coloring (GC) problems, including social network analysis [46], register allocation [47], network scheduling [48], and video processing [49].

REFERENCES

[1] H. Al-Hraishawi *et al.*, "A survey on nongeostationary satellite systems: The communication perspective," *IEEE Commun. Surv. Tutor.*, vol. 25, no. 1, pp. 101–132, 2023.

[2] X. Lin *et al.*, "On the path to 6g: Embracing the next wave of low earth orbit satellite access," *IEEE Commun. Mag.*, vol. 59, no. 12, pp. 36–42, 2021.

[3] N. Pachler de la Osa *et al.*, "Static beam placement and frequency plan algorithms for *LEO* constellations," *Int. J. Satellite Commun. Netw.*, vol. 39, no. 1, pp. 65–77, 2021.

[4] R. A. Dianez, "Joint optimization of beam placement and shaping for multi-beam high throughput satellite systems using gradient descent," Ph.D. dissertation, Universitat Politècnica de Catalunya, 2020.

[5] P. J. Honnaiah *et al.*, "Demand-driven beam densification in multibeam satellite communication systems," *IEEE Trans. Aerosp. Electron. Syst.*, vol. 59, no. 5, pp. 6534–6554, 2023.

[6] R. M. Karp, "Reducibility among combinatorial problems," in *Complexity of Computer Computations*, ser. The IBM Research Symposia Series, R. E. Miller and J. W. Thatcher, Eds., 1972, pp. 85–103.

[7] K. Bharti *et al.*, "Noisy intermediate-scale quantum algorithms," *Rev. Mod. Phys.*, vol. 94, p. 015004, Feb 2022.

[8] L. K. Grover, "A fast quantum mechanical algorithm for database search," in *Proc. 28th Annu. ACM Symp. Theory Comput.*, 1996, pp. 212–219.

[9] P. W. Shor, "Algorithms for quantum computation: discrete logarithms and factoring," in *Proc. 35th Annu. Symp. Found. Comput. Sci.*, 1994, pp. 124–134.

[10] E. Pelofske, A. Bärtschi, and S. Eidenbenz, "Quantum volume in practice: What users can expect from nisq devices," *arXiv*, 2022. [Online]. Available: https://arxiv.org/abs/2203.03816

[11] D-Wave, "D-Wave hybrid solver service: An overview," https://www.dwavesys.com/solutions-and-products/systems/, 2020.

[12] P. Hauke *et al.*, "Perspectives of quantum annealing: Methods and implementations," *Rep. Prog. Phys.*, vol. 83, no. 5, p. 054401, 2020.

[13] A. Lucas, "Ising formulations of many np problems," *Front. Phys.*, vol. 2, 2014.

[14] M. Kuramata, R. Katsuki, and K. Nakata, "Larger sparse quadratic assignment problem optimization using quantum annealing and a bit-flip heuristic algorithm," in *Proc. 8th IEEE Int. Conf. Ind. Eng. Appl. (ICIEA)*, Chengdu, China, Apr. 2021, pp. 556–565.

[15] D-Wave, "Upper limit for an arbitrary Ising problem on D-Wave," 2019. [Online]. Available: https://github.com/aws/amazon-braket-examples/.../Running_large_problem_using_QBSolv.ipynb

[16] T. Boothby, A. D. King, and A. Roy, "Fast clique minor generation in chimera qubit connectivity graphs," *Quantum Inf. Process.*, vol. 15, pp. 495–508, 2016.

[17] C. Rother *et. al.*, "Optimizing binary *MRFs* via extended *Roof Duality*," in *Proc. IEEE/CVF Conf. Comput. Vis. Pattern Recognit. (CVPR)*, Minneapolis, MN, USA, 2007, pp. 1–8.

[18] P. Thai *et. al.*, "Fasthare: Fast *Hamiltonian Reduction* for large-scale quantum annealing," in *Proc. 3rd IEEE Int. Conf. Quantum Comput. Eng. (QCE)*, Broomfield, CO, USA, Sep. 2022.

[19] G. E. Crooks, "Performance of the quantum approximate optimization algorithm on the maximum cut problem," *arXiv preprint arXiv:1811.08419*, 2018.

[20] L. Zhou, S.-T. Wang, S. Choi, H. Pichler, and M. D. Lukin, "Quantum approximate optimization algorithm: Performance, mechanism, and implementation on near-term devices," *Physical Review X*, vol. 10, no. 2, p. 021067, 2020.

[21] J. Li, M. Alam, and S. Ghosh, "Large-scale quantum approximate optimization via divide-and-conquer," *IEEE Trans. Comput.-Aided Des. Integr. Circuits Syst.*, vol. 42, no. 6, pp. 1852–1860, 2023.

[22] N. Hong, H. Jung, H. Kang, H. Lim, C. Seol, and S. Um, "A degree reduction method for an efficient qubo formulation for the graph coloring problem," *arXiv preprint arXiv:2306.12081*, 2023.

[23] 3rd Generation Partnership Project (3GPP), "TR 38.811: Study on New Radio (NR) to support non-terrestrial networks," 3rd Generation Partnership Project (3GPP), Technical Report 38.811, Jun. 2019, Technical Specification Group Radio Access Network; Release 15.

[24] T. S. Abdu *et al.*, "Flexible resource optimization for geo multibeam satellite communication system," *IEEE Trans. Wireless Commun.*, vol. 20, no. 12, pp. 7888–7902, 2021.

[25] A. Paris *et al.*, "A genetic algorithm for joint power and bandwidth allocation in multibeam satellite systems," in *Proc. IEEE Aerosp. Conf.*, Mar. 2019, pp. 1–15.

[26] V. P. Bui *et. al.*, "Joint beam placement and load balancing optimization for *Non-Geo*stationary satellite systems," in *Proc. IEEE MeditCom*, Athens, Greece, Sep. 2022.

[27] N. Pachler *et al.*, "Allocating power and bandwidth in multibeam satellite systems using particle swarm optimization," in *Proc. IEEE Aerosp. Conf.*, Mar. 2020, pp. 1–11.

[28] J. M. Keil and L. Stewart, "Approximating the minimum clique cover and other hard problems in subtree filament graphs," *Discret. Appl. Math.*, vol. 154, no. 14, pp. 1983–1995, 2006.

[29] M. Bellare, O. Goldreich, and M. Sudan, "Free bits, PCPs and non-approximability-towards tight results," in *Proc. IEEE Annu. Found. Comput. Sci.*, Milwaukee, WI, USA, 1995, pp. 422–431.

[30] X. Yuan, F. Tang, M. Zhao, and N. Kato, "Joint rate and coverage optimization for the thz/rf multi-band communications of space-air-ground integrated network in 6g," *IEEE Trans. Wireless Commun.*, vol. 23, no. 6, pp. 6669–6682, 2024.

[31] S. Cakaj, "The parameters comparison of the "Starlink"' LEO satellites constellation for different orbital shells," *Front. Commun. Netw.*, vol. 2, p. 643095, 2021.

[32] Z. Zhao, L. Fan, and Z. Han, "Hybrid quantum benders' decomposition for mixed-integer linear programming," in *2022 IEEE Wireless Communications and Networking Conference (WCNC)*, 2022, pp. 2536–2540.

[33] C. Gambella and A. Simonetto, "Multiblock admm heuristics for mixed-binary optimization on classical and quantum computers," *IEEE Trans. Quantum Eng.*, vol. 1, pp. 1–22, 2020.

[34] E. Pelofske, G. Hahn, and H. N. Djidjev, "Solving larger maximum clique problems using parallel quantum annealing," *Quantum Inf. Process.*, vol. 22, no. 5, p. 219, 2023.

[35] F. Glover, G. Kochenberger, R. Hennig, and Y. Du, "Quantum bridge analytics I: a tutorial on formulating and using QUBO models," *Ann. Oper. Res.*, vol. 314, no. 1, pp. 141–183, 2022.

[36] J. J. Berwald, "The mathematics of quantum-enabled applications on the d-wave quantum computer," *Not. Am. Math. Soc.*, vol. 66, no. 6, 2019.

[37] R. Boppana and M. M. Halldórsson, "Approximating maximum independent sets by excluding subgraphs," *BIT Numer. Math.*, vol. 32, no. 2, pp. 180–196, 1992.

[38] J. A. Nelder and R. Mead, "A simplex method for function minimization," *Comput. J.*, vol. 7, no. 4, pp. 308–313, 1965.

[39] U.S. Coast Guard, "Vessel Traffic data," https://marinecadastre.gov/ais/.

[40] D-Wave, "Operation and timing," D-Wave, Tech. Rep., accessed on Jul. 2023. [Online]. Available: https://docs.dwavesys.com/docs/latest/c_qpu_timing.html

[41] A. Silberschatz, P. B. Galvin, and G. Gagne, *Operating System Concepts, 10e Abridged Print Companion*. John Wiley & Sons, 2018.

[42] C. Bron and J. Kerbosch, "Algorithm 457: finding all cliques of an undirected graph," *Commun. ACM*, vol. 16, no. 9, pp. 575–577, 1973.

[43] V. Bhosale, A. Saeed, K. Bhardwaj, and A. Gavrilovska, "A Characterization of Route Variability in LEO Satellite Networks," in *Springer PAM*, 2023, pp. 313–342.

[44] G. Palubeckis, "Multistart tabu search strategies for the unconstrained binary quadratic optimization problem," *Ann. Oper. Res.*, vol. 131, pp. 259–282, 2004.

[45] S. Kirkpatrick, C. D. Gelatt Jr, and M. P. Vecchi, "Optimization by simulated annealing," *Science*, vol. 220, no. 4598, pp. 671–680, 1983.

[46] A. Conte, R. Grossi, and A. Marino, "Large-scale clique cover of real-world networks," *Inf. Comput.*, vol. 270, p. 104464, 2020.
[47] G. J. Chaitin, "Register allocation & spilling via graph coloring," *ACM Sigplan Not.*, vol. 17, no. 6, pp. 98–101, 1982.
[48] S. H. Cheng and C. Y. Huang, "Coloring-based inter-wban scheduling for mobile wireless body area networks," *IEEE Trans. Parallel Distrib. Syst.*, vol. 24, no. 2, pp. 250–259, 2013.
[49] D. Zhang, O. Javed, and M. Shah, "Video object co-segmentation by regulated maximum weight cliques," in *Proc. Eur. Conf. Comput. Vis. (ECCV)*. Zurich, Switzerland: Springer, Sep. 2014, pp. 551–566.

Thinh Quang Dinh (Member, IEEE) received the B.Eng. degree (Hons.) in electrical and electronic engineering (specializing in telecommunications) from the Ho Chi Minh City University of Technology (HCMUT), Vietnam, in 2013, and the Ph.D. degree from the Singapore University of Technology and Design (SUTD) in 2019 under the President's Graduate Fellowship. In 2018, he was a Visiting Student with the Wireless Computing Laboratory, University of Toronto. In 2019, he was a Data Scientist with Trusting Social. He was honored with the 2020 IEEE Stephen O. Rice Prize. His research interests include both quantum and classical communication systems and networking.

Son Hoang Dau (Hoang) (Member, IEEE) received the B.S. degree in applied mathematics and informatics from Vietnam National University, Hanoi, Vietnam, in 2006, and the M.S. and Ph.D. degrees in mathematical sciences from Nanyang Technological University, Singapore, in 2008 and 2012, respectively. He worked as a research fellow at Singapore University of Technology and Design (8/2012-8/2015), University of Illinois at Urbana-Champaign (8/2015-8/2017), and Monash University (11/2017-1/2019), before joining RMIT University in 2019. He is currently a senior lecturer in Computer Science at School of Computing Technologies, STEM College, RMIT University. His research interests include coding theory, blockchain, and discrete mathematics.

Eva Lagunas (Senior Member, IEEE) received the M.Sc. and Ph.D. degrees in telecommunications engineering from the Polytechnic University of Catalonia (UPC), Barcelona, Spain, in 2010 and 2014, respectively. She has held positions at UPC, Centre Tecnologic de Telecomunicacions de Catalunya (CTTC), University of Pisa, Italy; and the Center for Advanced Communications (CAC), Villanova University, PA, USA. In 2014, she joined the Interdisciplinary Centre for Security, Reliability and Trust (SnT), University of Luxembourg, where she currently holds a Research Scientist position. Her research interests include terrestrial and satellite system optimization, spectrum sharing, resource management and machine learning.

Symeon Chatzinotas (Fellow, IEEE) is currently Full Professor / Chief Scientist I and Head of the research group SIGCOM in the Interdisciplinary Centre for Security, Reliability and Trust, University of Luxembourg. In parallel, he is an Adjunct Professor in the Department of Electronic Systems, Norwegian University of Science and Technology and a Collaborating Scholar of the Institute of Informatics & Telecommunications, National Center for Scientific Research "Demokritos".

He has received the M.Eng. in Telecommunications from Aristotle University of Thessaloniki, Greece and the M.Sc. and Ph.D. in Electronic Engineering from University of Surrey, UK in 2003, 2006 and 2009 respectively.

He has authored more than 800 technical papers in refereed international journals, conferences and scientific books and has received numerous awards and recognition, including an IEEE Distinguished Contributions Award. He has served in the editorial board of the IEEE Transactions on Communications, IEEE Open Journal of Vehicular Technology and the International Journal of Satellite Communications and Networking.

Diep N. Nguyen (Senior Member, IEEE) received the M.E. degree in electrical and computer engineering from the University of California at San Diego (UCSD), La Jolla, CA, USA, in 2008, and the Ph.D. degree in electrical and computer engineering from The University of Arizona (UA), Tucson, AZ, USA, in 2013. He is currently the Head of 5G/6G Wireless Communications and Networking Lab, Director of Agile Communications and Computing group, Faculty of Engineering and Information Technology, University of Technology Sydney (UTS), Sydney, Australia. Before joining UTS, he was a DECRA Research Fellow with Macquarie University, Macquarie Park, NSW, Australia, and a Member of the Technical Staff with Broadcom Corporation, CA, USA, and ARCON Corporation, Boston, MA, USA, and consulting the Federal Administration of Aviation, Washington, DC, USA, on turning detection of UAVs and aircraft, and the U.S. Air Force Research Laboratory, USA, on anti-jamming. His research interests include computer networking, wireless communications, and machine learning application, with emphasis on systems' performance and security/privacy. Dr. Nguyen received several awards from LG Electronics, UCSD, UA, the U.S. National Science Foundation, and the Australian Research Council. He has served on the Editorial Boards of the IEEE Transactions on Mobile Computing, IEEE Communications Surveys & Tutorials (COMST), IEEE Open Journal of the Communications Society.

Dinh Thai Hoang (Senior Member, IEEE) is currently a faculty member at the School of Electrical and Data Engineering, University of Technology Sydney, Australia. He received his Ph.D. in Computer Science and Engineering from the Nanyang Technological University, Singapore 2016. His research interests include emerging wireless communications and networking topics, especially machine learning applications in networking, edge computing, and cybersecurity. He has received several precious awards, including the Australian Research Council Discovery Early Career Researcher Award, IEEE TCSC Award for Excellence in Scalable Computing for Contributions on "Intelligent Mobile Edge Computing Systems" (Early Career Researcher), IEEE Asia-Pacific Board (APB) Outstanding Paper Award 2022, and IEEE Communications Society Best Survey Paper Award 2023. He is currently an Editor of IEEE TMC, IEEE TWC, and IEEE TNSE.